arXiv:1208.1637v1 [cond-mat.quant-gas] 8 Aug 2012

Effects of Rashba and Dresselhaus spin-orbit couplings on singlet and triplet condensation with Fermi atoms

L. Dell'Anna, G. Mazzarella, and L. Salasnich
Dipartimento di Fisica "Galileo Galilei" and CNISM, Università di Padova, Italy

We investigate the pair condensation of a two-spin-component Fermi gas in the presence of both Rashba and Dresselhaus spin-orbit couplings. We calculate the condensate fraction in the BCS-BEC crossover both in two and in three dimensions by taking into account singlet and triplet pairings. These quantities are studied by varying the spin-orbit interaction from the case with the only Rashba to the equal-Rashba-Dresselhaus one. We find that, by mixing the two couplings, the singlet pairing decreases while the triplet pairing is suppressed in the BCS regime and increased in the BEC regime, both in two and three dimensions. At fixed spin-orbital strength, the greatest total condensate fraction is obtained when only one coupling (only Rashba or only Dresselhaus) is present.

PACS numbers: 03.75.Ss, 05.30.Fk, 67.85.Lm

I. INTRODUCTION

In the last years the predicted crossover [1–3] from the Bardeen-Cooper-Schrieffer (BCS) state of weakly bound Fermi pairs to the Bose-Einstein condensate (BEC) of molecular dimers has been observed by several experimental groups [4–9]. In particular, two seminal experiments [7, 9], with two hyperfine component Fermi vapours of ^{6}Li atoms in the BCS-BEC crossover, have been performed to study the condensate fraction of Cooper pairs [10], which is directly related to the off-diagonal-long-range order of the two-body density matrix of fermions [11, 12]. At very low temperature these experimental results show an excellent agreement with the zero-temperature theoretical predictions of mean-field approaches [13, 14] and Monte-Carlo simulations [15]. However, as discussed in [16], when the effects of temperature cannot be neglected it is necessary to include beyond mean-field corrections to reproduce quantitatively the experimental data. Intensive theoretical studies have been developed on the condensate fraction along BCS-BEC crossover for a two-dimensional (2D) Fermi gas [17–22], and for a three-spin-component Fermi gas with SU(3) symmetry [23–25] as well. The recent experimental realization of 2D degenerate Fermi gases for ultra-cold atoms in a highly anisotropic disk-shaped potential [26] is one of the reasons of the growing interest for fermions in reduced dimensionality.

Very recently artificial spin-orbit coupling has been realized in neutral bosonic systems [27]. In such systems the strength of the coupling can be optically tuned and this is indeed a useful tool also for ultracold fermions [28, 29]. These achievements have stimulated theoretical efforts in understanding the spin-orbit effects with Rashba [30] and Dresselhaus [31] terms in the BCS-BEC crossover [32–49]. The evolution from BCS to BEC superfluidity was intensively studied in the presence of spin-orbit coupling for a 3D uniform Fermi gas [33–40, 42, 43, 45] and in the 2D case [39, 41, 44–46, 49]. In Ref. [39] we have analyzed the effects of the spin-orbit coupling on the condensate fraction by studying both the singlet and the triplet pairing contributions in the presence of the Rashba coupling.

In this paper we extend and complete the zero-temperature study presented in [39]. In particular we investigate the condensate fraction along the BCS-BEC crossover with Rashba and Dresselhaus spin-orbit couplings both in 2D and in 3D analyzing singlet and triplet contributions to pairing condensation. We study these quantities at zero temperature by gradually including the effect of the Dresselhaus term in the spin-orbit coupling. We show that along this tuning the singlet contribution to the condensate fraction always decreases, while the triplet contribution is strongly suppressed in the BCS regime and enhanced in the BEC one, both in 2D and in 3D. Indeed this enhancement in 2D takes place when the binding energy is greater than the Fermi energy and in 3D when the dimensionless interaction parameter $y = 1/(k_F a_s)$ (k_F is the Fermi linear momentum and a_s the interatomic s-wave scattering length) is mainly positive. We find that the total condensate fraction is greater when only the Rashba coupling is active. Instead, when the Rashba and Dresselhaus couplings are equal the total condensate fraction is the same as that obtained in the absence of spin-orbit coupling. The chemical potential and the pairing gap decrease in both the two regimes, when the coupling is changed from the only-Rashba to equal-Rashba-Dresselhaus case.

II. THE MODEL

We describe a gas of two-spin-component Fermi atoms with spin-orbit couplings [30, 31] by using the following one-body Hamiltonian

$$
\begin{aligned}
H_0 \;&=\; \sum_{\mathbf{k}} \psi(\mathbf{k})^\dagger \Big\{ \frac{\hbar^2 k^2}{2m} - \mu + \hbar\big[v_R(\sigma_x k_y - \sigma_y k_x) \\
&+\; v_D(\sigma_x k_y + \sigma_y k_x) \big] \Big\} \psi(\mathbf{k}) \,, \qquad (1)
\end{aligned}
$$

where μ is the chemical potential and v_D and v_R are, respectively, the Rashba and Dresselhaus velocities; σ_x and σ_y denote the Pauli matrices in the x and y directions, and $\psi(\mathbf{k}) = (\psi_\uparrow(\mathbf{k}), \psi_\downarrow(\mathbf{k}))^T$ is the Nambu spinor. Notice that we can rewrite Eq. (1) as

$$H_0 = \sum_{\mathbf{k}} \psi(\mathbf{k})^\dagger \left[\frac{\hbar^2}{2m} \left(\vec{k} + \vec{A} \right)^2 - (\mu + mv^2) \right] \psi(\mathbf{k}) \ , \tag{2}$$

where

$$\begin{aligned} v_R &= v \cos\theta & (3) \\ v_D &= v \sin\theta & (4) \\ \vec{A} &= \frac{mv}{\hbar} \begin{pmatrix} (\sin\theta - \cos\theta)\sigma_y \\ (\sin\theta + \cos\theta)\sigma_x \\ 0 \end{pmatrix} \ . & (5) \end{aligned}$$

In addition to the one-body Hamiltonian H_0 we consider the two-body interaction Hamiltonian given by

$$H_I = -\frac{g}{V} \sum_{\mathbf{k}\mathbf{k}'\mathbf{q}} \psi_\uparrow^\dagger(\mathbf{k}+\mathbf{q}) \psi_\downarrow^\dagger(-\mathbf{k}) \psi_\downarrow(-\mathbf{k}'+\mathbf{q}) \psi_\uparrow(\mathbf{k}') \ , \tag{6}$$

where $g > 0$, which corresponds to attractive interaction. The total Hamiltonian thus reads

$$H = H_0 + H_I \ . \tag{7}$$

From this Hamiltonian we calculate the effects of Rashba and Dresselhaus spin-orbit couplings on singlet and triplet condensation with Fermi atoms in the full BCS-BEC crossover.

III. GAP ORDER PARAMETER AND CONDENSATES

By decoupling at the mean-field level the two-body interaction (6) we get

$$H_I = V \frac{|\Delta|^2}{g} - \sum_{\mathbf{k}} \left(\Delta^* \psi_\downarrow(-\mathbf{k}) \psi_\uparrow(\mathbf{k}) + \Delta \psi_\uparrow^\dagger(\mathbf{k}) \psi_\downarrow^\dagger(-\mathbf{k}) \right) \ , \tag{8}$$

where V is the volume and

$$\Delta = (g/V) \sum_{\mathbf{k}} \langle \psi_\downarrow(-\mathbf{k}) \psi_\uparrow(\mathbf{k}) \rangle \tag{9}$$

is the familiar gap order parameter describing the correlation energy of singlet Cooper pairs.

As discussed in [39], from the Hamiltonian (7) with H_0 given by Eq. (2) and H_I by Eq. (8) we can calculate the spectrum of single-particle elementary excitations, which is given by

$$\begin{aligned} E_1(\mathbf{k}) &= \sqrt{(\xi_{\mathbf{k}} - |\gamma(\mathbf{k})|)^2 + |\Delta|^2} & (10) \\ E_2(\mathbf{k}) &= \sqrt{(\xi_{\mathbf{k}} + |\gamma(\mathbf{k})|)^2 + |\Delta|^2} & (11) \\ E_3(\mathbf{k}) &= -E_1(\mathbf{k}) & (12) \\ E_4(\mathbf{k}) &= -E_2(\mathbf{k}) & (13) \end{aligned}$$

with

$$\gamma(\mathbf{k}) = \hbar v_R (k_y + i k_x) + \hbar v_D (k_y - i k_x) \tag{14}$$

and

$$\xi_{\mathbf{k}} = \hbar^2 k^2 / 2m - \mu \ . \tag{15}$$

Moreover, the number of particles reads

$$N = \sum_{\mathbf{k}} \left\{ 1 - \frac{\xi_{\mathbf{k}} - |\gamma(\mathbf{k})|}{2E_1(\mathbf{k})} - \frac{\xi_{\mathbf{k}} + |\gamma(\mathbf{k})|}{2E_2(\mathbf{k})} \right\} , \tag{16}$$

while the energy gap Δ is obtained by solving the corresponding gap equation

$$\frac{V}{g} = \frac{1}{4} \sum_{\mathbf{k}} \left(\frac{1}{E_1(\mathbf{k})} + \frac{1}{E_2(\mathbf{k})} \right) \ . \tag{17}$$

In addition, the condensate number N_C [52] of Cooper pairs is given by

$$N_c = N_0 + N_1, \tag{18}$$

where

$$\begin{aligned} N_0 &= \sum_{\mathbf{k}} |\langle \psi_\uparrow(\mathbf{k}) \psi_\downarrow(-\mathbf{k}) \rangle|^2 & (19) \\ &= \frac{|\Delta|^2}{16} \sum_{\mathbf{k}} \left(\frac{1}{E_1(\mathbf{k})} + \frac{1}{E_2(\mathbf{k})} \right)^2 \end{aligned}$$

is the singlet, with total spin 0, contribution to the condensate, whereas

$$\begin{aligned} N_1 &= \sum_{\mathbf{k}} |\langle \psi_\uparrow(\mathbf{k}) \psi_\uparrow(-\mathbf{k}) \rangle|^2 & (20) \\ &= \frac{|\Delta|^2}{16} \sum_{\mathbf{k}} \left(\frac{1}{E_1(\mathbf{k})} - \frac{1}{E_2(\mathbf{k})} \right)^2 \end{aligned}$$

is the triplet one, with total spin 1. Eqs. (16), (17), (19) and (20) are the starting point of our present investigation. The finite-temperature version of these equations can be found in our previous paper [39]. It is important to notice that, even if at the mean-field level only the singlet energy gap $\Delta = \Delta_{\downarrow\uparrow}$ appears, while the triplet one, $\Delta_{\uparrow\uparrow} = (g/V) \sum_{\mathbf{k}} \langle \psi_\uparrow(-\mathbf{k}) \psi_\uparrow(\mathbf{k}) \rangle$, is absent, as one can see from Eq. (6), triplet pairing can be generated by the presence of the spin-orbital interaction.

We study our system both in two dimensional (2D) and in three dimensional (3D) case in the absence of the temperature, $T = 0$. With this purpose, we have to analyze the key quantities for the 2D case - the binding energy ϵ_B, the condensate densities n_S ($S = 0$ for the singlet and $S = 1$ for the triplet), the chemical potential μ, and the gap Δ - and for the 3D case - the interaction parameter y, the condensate densities n_S, the chemical potential μ, and the gap Δ. We follow the same path as in [39], that is we define the dimensionless parameters

$$x_0 = \frac{\mu}{\Delta} \tag{21}$$

$$x_1 = 2m\frac{(v_R - v_D)^2}{\Delta} = \frac{2mv^2}{\Delta}(1 - \sin 2\theta) \tag{22}$$

$$x_2 = 2m\frac{(v_R + v_D)^2}{\Delta} = \frac{2mv^2}{\Delta}(1 + \sin 2\theta) \tag{23}$$

so that for the 2D case we have

$$\frac{\epsilon_B}{\Delta} = \lim_{\Lambda\to\infty} \frac{2\Lambda^2}{\exp[I_g(x_0, x_1, x_2)/\pi] - 1} \tag{24}$$

$$\frac{2n_S}{n} = \frac{1}{8}\frac{I^2_{N_S}(x_0, x_1, x_2)}{I^2_N(x_0, x_1, x_2)} \tag{25}$$

$$\frac{\mu}{\epsilon_F} = \frac{2\pi x_0}{I^2_N(x_0, x_1, x_2)} \tag{26}$$

$$\frac{\Delta}{\epsilon_F} = \frac{2\pi}{I^2_N(x_0, x_1, x_2)} \tag{27}$$

$$\frac{(v_R \mp v_D)^2}{v_F^2} = \frac{\pi}{2}\frac{x_{1,2}}{I^2_N(x_0, x_1, x_2)} \tag{28}$$

with Λ the ultraviolet momentum cut-off. For the 3D, one has

$$y \equiv \frac{1}{k_F a_s} = \frac{1}{3^{1/3}\pi^{5/3}}\frac{I_{a_s}(x_0, x_1, x_2)}{I^3_N(x_0, x_1, x_2)^{1/3}} \tag{29}$$

$$\frac{2n_S}{n} = \frac{1}{8}\frac{I^3_{N_S}(x_0, x_1, x_2)}{I^3_N(x_0, x_1, x_2)} \tag{30}$$

$$\frac{\mu}{\epsilon_F} = 4\left(\frac{\pi}{3}\right)^{2/3} x_0 I^3_N(x_0, x_1, x_2)^{-2/3} \tag{31}$$

$$\frac{\Delta}{\epsilon_F} = 4\left(\frac{\pi}{3}\right)^{2/3} I^3_N(x_0, x_1, x_2)^{-2/3} \tag{32}$$

$$\frac{(v_R \mp v_D)^2}{v_F^2} = \left(\frac{\pi}{3}\right)^{2/3} x_{1,2}\, I^3_N(x_0, x_1, x_2)^{-2/3} \tag{33}$$

with k_F the Fermi wave vector and a_s the interatomic s-wave scattering length. All the above equations are written in terms of the following dimensionless integrals:

$$\begin{aligned}
I_g(x_0, x_1, x_2) &= \frac{1}{2}\int^{\Lambda} d^2\mathbf{q} \sum_{r=\pm1} \frac{1}{\sqrt{\left(q^2 - x_0 + r\sqrt{x_1 q_x^2 + x_2 q_y^2}\right)^2 + 1}} \\
I^d_N(x_0, x_1, x_2) &= \int d^d\mathbf{q} \left(1 - \frac{1}{2}\sum_{r=\pm1} \frac{q^2 - x_0 + r\sqrt{x_1 q_x^2 + x_2 q_y^2}}{\sqrt{\left(q^2 - x_0 + r\sqrt{x_1 q_x^2 + x_2 q_y^2}\right)^2 + 1}}\right) \\
I^d_{N_S}(x_0, x_1, x_2) &= \int d^d\mathbf{q} \left(\sum_{r=\pm1} \frac{r^S}{\sqrt{\left(q^2 - x_0 + r\sqrt{x_1 q_x^2 + x_2 q_y^2}\right)^2 + 1}}\right)^2 \\
I_{a_s}(x_0, x_1, x_2) &= \int d^3\mathbf{q} \left(\frac{1}{q^2} - \frac{1}{2}\sum_{r=\pm1} \frac{1}{\sqrt{\left(q^2 - x_0 + r\sqrt{x_1 q_x^2 + x_2 q_y^2}\right)^2 + 1}}\right) ,
\end{aligned} \tag{34}$$

where $d = 2$ holds for the 2D case, while $d = 3$ for the 3D one; $S = 0$ for the singlet and $S = 1$ for the triplet contribution.

IV. RESULTS

In Fig. 1 we plot the condensate fraction of the 2D Fermi system as a function of the scaled binding energy ϵ_B/ϵ_F, with ϵ_F the 2D Fermi energy, for different values of the characteristic velocity $v = \sqrt{v_R^2 + v_D^2}$ and two values of the mixing angle $\theta = \arctan(v_D/v_R)$. In the first two panels there are the singlet (top panel) and triplet (middle panel) contributions to the condensate fraction, while in the lower panel there is the total condensate fraction. The results are shown for $\theta = 0$ ($v_D = 0$, solid curves) and $\theta = \pi/4$ ($v_R = v_D$, dashed curves) and three values of the velocity v.

In Fig. 2 we plot instead the condensate fraction of the 3D Fermi system as a function of the scaled interaction strength $y = 1/(k_F a_s)$ with k_F the 3D Fermi linear momentum and a_s the s-wave scattering length. As in Fig.

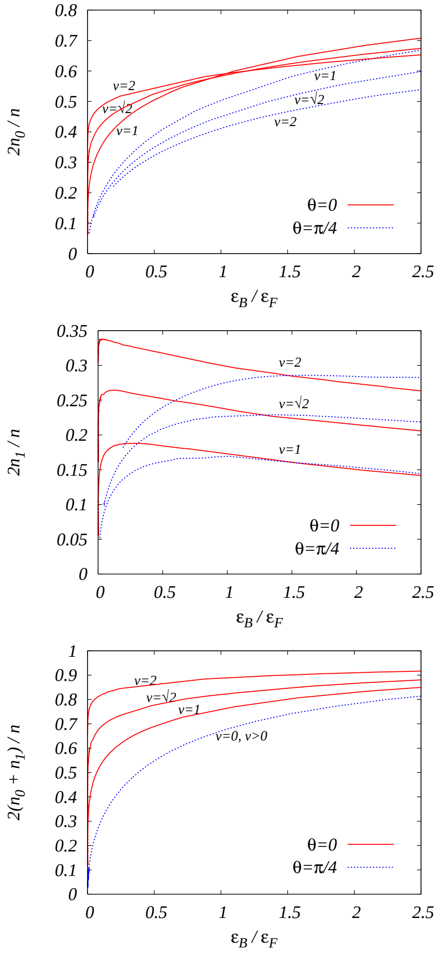

FIG. 1: (Color online) 2D Fermi superfluid. Singlet (top panel) and triplet (middle panel) contributions to the condensate fraction for $v^2 = 1, 2, 4$ (in units of v_F^2) and for $\theta = 0$, i.e. only Rashba term, (red solid curves) and $\theta = \pi/4$, i.e. for equal Rashba and Dresselhaus terms, (blue dashed line). Bottom panel: the total condensate fraction, i.e. the sum of both singlet and triplet contributions, for the same values of v and θ. Notice that for $\theta = \pi/4$ (blue dashed line), the full condensate fraction is the same as without spin-orbit ($v = 0$).

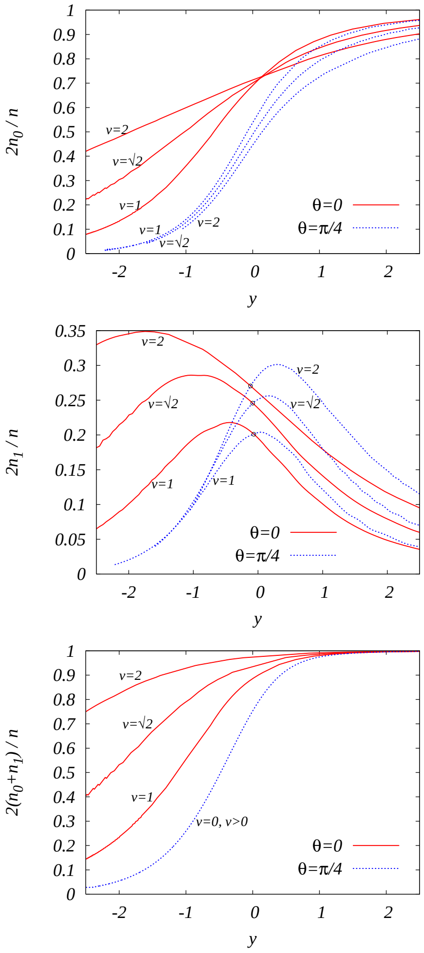

FIG. 2: (Color online) 3D Fermi superfluid. Singlet (top panel) and triplet (middle panel) contributions to the condensate fraction for $v^2 = 1, 2, 4$ (in units of v_F^2) and for $\theta = 0$, i.e. only Rashba term, (red solid curves) and $\theta = \pi/4$, i.e. for equal Rashba and Dresselhaus terms, (blue dashed line). Bottom panel: the total condensate fraction, i.e. the sum of both singlet and triplet contributions, for the same values of v and θ. Notice that for $\theta = \pi/4$ (blue dashed line), the full condensate fraction is the same as without spin-orbit ($v = 0$).

1 in the first two panels there are the singlet (top panel) and triplet (middle panel) contributions to the condensate fraction, while in the lower panel there is the total condensate fraction. Again, results are shown for $\theta = 0$ ($v_D = 0$, solid curves) and $\theta = \pi/4$ ($v_R = v_D$, dashed curves) and three values of the velocity v. The two sets of plots corresponding to 2D and 3D share many features and would have looked very similar if we had plotted Fig. 1 in terms of $\ln(1/k_F a_{2D}) \equiv \ln(\epsilon_B/2\epsilon_F)/2$.

Our calculations show that the singlet contribution to the condensate fraction, $2n_0/n$, both in 2D and in 3D, decreases when one fixes v/v_F and moves from the only-Rashba (or only-Dresselhaus) case ($\theta = 0$) to equal-Rashba-Dresselhaus case ($\theta = \pi/4$), as it can be observed from the top panels of Figs. 1 and 2. In the case of only Rashba ($\theta = 0$) we observed [39] that, for one value of the scattering parameter close to the crossover ($\epsilon_B \simeq \epsilon_F$ in 2D and $y \simeq 0$ in 3D) and for $v \gtrsim v_F$, n_0/n does not depends on v, namely there is a nodal point for the singlet condensate fraction when one increases largely enough the Rashba coupling, see red solid curves in the top panels of Figs. 1 and 2. Regarding the triplet contribution, $2n_1/n$, we find that for sufficiently small values of the binding energy ϵ_B/ϵ_F (in 2D) or for $y < 0$ (in 3D), $2n_1/n$ is suppressed by mixing the two spin-orbital couplings, whereas when ϵ_B/ϵ_F (in 2D) becomes large enough ($\epsilon_B \gtrsim 1.5\epsilon_F$) and $y \gtrsim 0$ (in 3D), the triplet contribution is enhanced, see the middle panels of Figs. 1 and 2. The full condensate fraction, $n_C/n = 2(n_0 + n_1)/n$, at fixed v/v_F, is maximum for only-Rashba (or only-Dresselhaus) case ($\theta = 0$). In the extreme case of equal Rashba and Dresselhaus contribu-

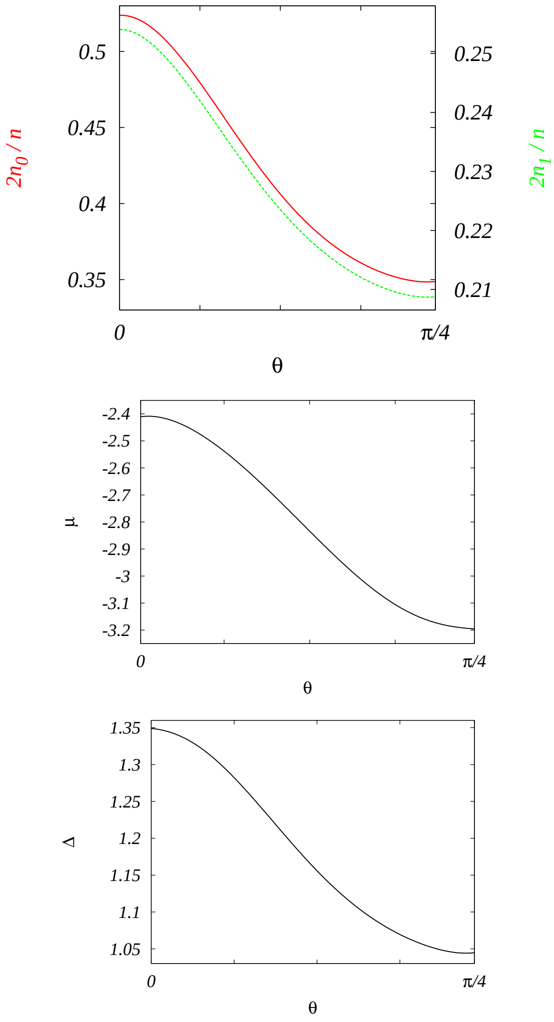

FIG. 3: (Color online) 2D Fermi superfluid. Top panel: Singlet (red solid line, left y-axis) and triplet (green dashed line, right y-axis) contributions to the condensate fraction, for $v^2 = 2v_F^2$ and $\epsilon_B = 0.5\epsilon_F$, as functions of θ. Notice that $2n_0/n$ and $2n_1/n$ are plotted with different scales. Middle panel: chemical potential, μ (in units of ϵ_F), for $v^2 = 2v_F^2$ and $\epsilon_B = 0.5\epsilon_F$, as a function of θ. Bottom panel: gap function, Δ (in units of ϵ_F), for $v^2 = 2v_F^2$ and $\epsilon_B = 0.5\epsilon_F$, as a function of θ.

tions ($\theta = \pi/4$), instead, the total condensate fraction is the same as that obtained without spin-orbit at all, i.e. with $v = 0$, see the dotted line of the bottom panels of Figs. 1 and 2. In particular, for the case of $\theta = \pi/4$ the following results for the condensate fraction, the chemical potential and the gap function hold

$$\frac{n_c}{n}(v, \theta = \pi/4) = \frac{n_c}{n}(v = 0) \tag{35}$$

$$\mu(v, \theta = \pi/4) = \mu(v = 0) - mv^2 \tag{36}$$

$$\Delta(v, \theta = \pi/4) = \Delta(v = 0)\ . \tag{37}$$

The chemical potential is consistent with the known perturbative result for small v and small ϵ_B, which is $\mu \simeq \epsilon_F - mv^2$. In the case of $\theta = \pi/4$, Eq.(36) is valid for all values of the binding energy ϵ_B and comes simply from gauge transforming the fields, $\psi(\mathbf{r}) \to e^{iyA_y}\psi(\mathbf{r})$, in the Hamiltonian Eq. (2).

Let us now investigate in detail the condensate fractions n_0/n and n_1/n, the chemical potential μ and the energy gap Δ when θ is increased from 0 to $\pi/4$. For computational simplicity, we consider the two dimensional case.

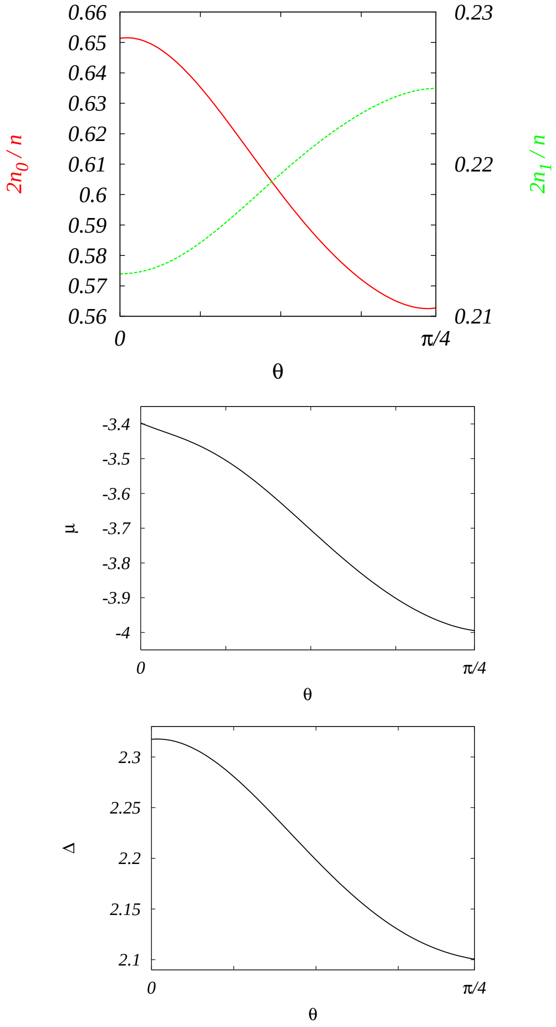

FIG. 4: (Color online) 2D Fermi superfluid. Top panel: Singlet (red solid line, left y-axis) and triplet (green dashed line, right y-axis) contributions to the condensate fraction, for $v^2 = 2v_F^2$ and $\epsilon_B = 2\epsilon_F$, as functions of θ. Middle panel: chemical potential μ (in units of ϵ_F) for $v^2 = 2v_F^2$ and $\epsilon_B = 2\epsilon_F$, as a function of θ. Bottom panel: gap function, Δ (in units of ϵ_F), for $v^2 = 2v_F^2$ and $\epsilon_B = 2\epsilon_F$, as a function of θ.

In Figs. 3 and 4 we plot these quantities by choosing $v^2 = 2v_F^2$ in correspondence to two different values of the binding energy. These two binding energies are those for which a softening and a hardening of the triplet contribution ($2n_1/n$) against θ is expected; thus Fig. 3 is obtained with $\epsilon_B = 0.5\epsilon_F$ and Fig. 4 with $\epsilon_B = 2\epsilon_F$ (see the above discussion about Fig. 1). From the former figure, Fig. 3, it can be pointed out that, for small binding energies, $2n_1/n$ decreases by increasing θ from 0 to $\pi/4$, and the same behavior, but rescaled, is observed for the singlet contribution $2n_0/n$ (see the top panel). Both the chemical potential and the gap function decrease going from the only-Rashba case to a fully mixed one. Fig. 4, instead, shows that, for large binding energies, $2n_1/n$ increases when θ is changed from $\theta = 0$ to $\theta = \pi/4$, while $2n_0/n$ always decreases, as well as the chemical potential and the gap function. In both above discussed cases, the singlet contribution to the condensate fraction is always greater than the triplet one.

V. CONCLUSIONS

We have analyzed the condensation of fermionic atoms along the BCS-BEC crossover in the presence of Rashba and Dresselhaus spin-orbit couplings. The condensation has been characterized by calculating the singlet and the triplet contributions to the pairing and therefore the full condensate fraction. We have studied these quantities by varying the spin-orbit from the situation in which the only Rashba coupling is present to that in which the Rashba and Dresselhaus velocities are equal. We have found that moving along this path, the singlet contribution to the condensate fraction decreases, while the triplet one behaves differently in the two regimes (BCS and BEC). In the BCS regime, the triplet pairing is suppressed upon mixing the two spin-orbit couplings while in the BEC regime it experiences an enhancement over the only-Rashba case. In other words, the triplet pairing is maximized in the BCS regime if only Rashba (or only Dresselhaus) term is active, while it is strengthened in the BEC regime by mixing the two spin-orbital couplings. This behavior takes place both in two and three dimensions. We have shown also that the total condensate fraction is greater when only one coupling (only Rashba or only Dresselhaus) is present, while in the equal-Rashba-Dresselhaus case, is the same as that obtained without spin-orbit.

[1] D.M. Eagles, Phys. Rev. **186**, 456 (1969).

[2] A.J. Leggett, in *Modern Trends in the Theory of Condensed Matter*, p. 13, edited by A. Pekalski and J. Przystawa (Springer, Berlin, 1980).

[3] P. Noziers, S. Schmitt-Rink, J. Low Temp. Phys. **59**, 195 (1985).

[4] M. Greiner, C.A. Regal, and D.S. Jin, Nature (London) **426**, 537 (2003).

[5] C.A. Regal, M. Greiner, and D.S. Jin, Phys. Rev. Lett. **92**, 040403 (2004).

[6] J. Kinast, S.L. Hemmer, M.E. Gehm, A. Turlapov, J.E. Thomas, Phys. Rev. Lett. **92**, 150402 (2004).

[7] M.W. Zwierlein *et al.*, Phys. Rev. Lett. **92**, 120403 (2004); M.W. Zwierlein, C.H. Schunck, C.A. Stan, S.M.F. Raupach, W. Ketterle, Phys. Rev. Lett. **94**, 180401 (2005).

[8] C. Chin *et al.*, Science **305**, 1128 (2004); M. Bartenstein *et al.*, Phys. Rev. Lett. **92**, 203201 (2004).

[9] Y. Inada, M. Horikoshi, S. Nakajima, M. Kuwata-Gonokami, M. Ueda, and T. Mukaiyama, Phys. Rev. Lett. **101**, 180406 (2008).

[10] C.N. Yang, Rev. Mod. Phys. **34**, 694 (1962).

[11] O. Penrose, Phil. Mag. **42**, 1373 (1951); O. Penrose and L. Onsager, Phys. Rev. **104**, 576 (1956).

[12] C.E. Campbell, in Condensed Matter Theories, vol. **12**, 131 (Nova Science, New York, 1997).

[13] L. Salasnich, N. Manini, and A. Parola, Phys. Rev. A **72**, 023621 (2005).

[14] G. Ortiz and J. Dukelsky, Phys. Rev. A **72**, 043611 (2005).

[15] G. E. Astrakharchik, J. Boronat, J. Casulleras, and S. Giorgini, Phys. Rev. Lett. **93**, 200404 (2004).

[16] Y. Ohashi and A. Griffin, Phys. Rev. A **72**, 063606 (2005); N. Fukushima, Y. Ohashi, E. Taylor, and A. Griffin, Phys. Rev. A **75**, 033609 (2007).

[17] M. Marini, F. Pistolesi, G.C. Strinati, Eur. Phys. J. **1**, 151 (1998).

[18] L. Salasnich, Phys. Rev. A **76**, 015601 (2007).

[19] G. J. Conduit, P. H. Conlon and B. D. Simons, Phys. Rev. A **77**, 053617 (2008)

[20] L. He, and P. Zhuang, Phys. Rev. A **78**, 033613 (2008)

[21] J.J. Du, C. Chen, and J.J. Liang, Phys. Rev. A **80**, 023601 (2009)

[22] M.M. Parish, Phys. Rev. A **83**, 051603 (2011)

[23] T.N. De Silva, Phys. Rev. A **80**, 013620 (2009)

[24] L. Salasnich, Phys. Rev. A **83**, 033630 (2011).

[25] J. Du, J. Liang, J.-Q. Liang, arXiv:1202.5086.

[26] K. Martiyanov, V. Makhalov, and A. Turlapov, Phys. Rev. Lett. **105**, 030404 (2010).

[27] Y.J. Lin, K. Jimenez-Garcia, and I.B. Spielman, Nature **471**, 83 (2011).

[28] J. Dalibard, F. Gerbier, G. Juzeliunas, P. Ohberg, Rev. Mod. Phys. **83**, 1523 (2011).

[29] M. Chapman and C.A.R. Sa de Melo, Nature **471**, 41 (2011).

[30] Y.A. Bychkov and E.I. Rashba, J. Phys. C **17**, 6029 (1984).

[31] G. Dresselhaus, Phys. Rev. **100**, 580 (1955).

[32] J. P. Vyasanakere and V. B. Shenoy, Phys. Rev. B **83**, 094515 (2011).

[33] J. P. Vyasanakere, S. Zhang, and V. B. Shenoy, Phys. Rev. B **84**, 014512 (2011).

[34] M. Gong, S. Tewari, and C. Zhang, Phys. Rev. Lett. **107**, 195303 (2011).

[35] H. Hu, L. Jiang, X-J. Liu, and H. Pu, Phys. Rev. Lett. **107**, 195304 (2011).

[36] Z-Q. Yu and H. Zhai, Phys. Rev. Lett. **107**, 195305 (2011).

[37] M. Iskin and A. L. Subasi, Phys. Rev. Lett. **107**, 050402 (2011).

[38] W. Yi and G.-C. Guo, Phys. Rev. A **84**, 031608 (2011).

[39] L. Dell'Anna, G. Mazzarella, and L. Salasnich, Phys. Rev. A **84**, 033633 (2011).

[40] M. Iskin and A. L. Subasi, Phys. Rev. A **84**, 043621 (2011).

[41] J. Zhou, W. Zhang, and W. Yi, Phys. Rev. A, **84**, 063603 (2011).

[42] L. Jiang, X.-J. Liu, H. Hu, and H. Pu, Phys. Rev. A **84**, 063618 (2011).

[43] Li Han and C.A.R. Sa de Melo, Phys. Rev. A **85**, 011606(R) (2012).

[44] G. Chen, M. Gong, and C. Zhang, Phys. Rev. A **85**, 013601 (2012)

[45] K. Zhou, Z. Zhang, Phys. Rev. Lett. **108**, 025301 (2012).

[46] X. Yang, S. Wan, Phys. Rev. A **85**, 023633 (2012)

[47] M. Iskin, Phys. Rev. A **85**, 013622 (2012).

[48] K. Seo, L. Han, C.A.R. Sa de Melo, Phys. Rev. A **85**, 033601 (2012).

[49] L. He and Xu-Guang Huang, Phys. Rev. Lett. **108**, 145302 (2012).

[50] H.T.C. Stoof, B.M. Dennis, and K. Gubbels, *Ultracold Quantum Fields*, (Springer, Berlin, 2009).

[51] M. Randeria, J.-M. Duan, and L.-Y. Shieh, Phys. Rev. B **41**, 327 (1990).

[52] A. J. Leggett, *Quantum liquids*, Oxford University Press (New York, NY, USA, 2006).